Supporting Information

Laser-Scribed Graphene Electrodes Derived from Lignin for Biochemical Sensing

Yongjiu Lei, † *Aya H. Alshareef,* † *Wenli Zhao,* † *Sahika Inal**, ‡

† Materials Science and Engineering, Physical Science and Engineering Division, King Abdullah University of Science and Technology (KAUST), Thuwal 23955-6900, Saudi Arabia.

‡ Biological and Environmental Science and Engineering Division, King Abdullah University of Science and Technology (KAUST), Thuwal 23955-6900, Saudi Arabia

*E-mail: sahika.inal@kaust.edu.sa

Supplementary Text

Materials: Lignosulfonate (average Mw ~54,000, Sigma-Aldrich), polyvinyl alcohol (PVA, average Mw ~89000, Sigma-Aldrich), urea (99%, Sigma-Aldrich), acetic acid (≥99%, Sigma-Aldrich), glucose (≥99.5%, Sigma-Aldrich), lactate (≥99.0%, Sigma-Aldrich), ethanol (alcohol, ≥99.8%), chitosan (medium molecular weight, Sigma-Aldrich), acetic acid (99%, Sigma-Aldrich), glucose oxidase (2,07U/mg, Sigma-Aldrich), lactate oxidase (80 U/mg; Creative Enzymes, USA), alcohol oxidase (10-40 U/mg, Sigma-Aldrich), glutaraldehyde (25% in DI water, Sigma-Aldrich), potassium ferrocyanide ($K_4[Fe(CN)_6]$, 98%, Sigma-Aldrich), hexaaminruthenium(III) chloride ($[Ru(NH_3)_6]Cl_3$, 98%, Sigma-Aldrich), potassium chloride (99%, Sigma-Aldrich), ammonium chloride (≥ 99.5%, Sigma-Aldrich), sodium chloride (≥99.5%, Sigma-Aldrich).

Synthesis of $Ti_3C_2T_x$ nanosheets and $Ti_3C_2T_x$/PB nanocomposite

$Ti_3C_2T_x$ was prepared with the MILD method, whereby manual shaking of the etched $Ti_3C_2T_x$ powder suspension to achieve delamination of MXene. The etching solution was prepared by mixing 1mL of hydrofluoric acid (HF, sigma, 49.0%), 6 mL of 12 M hydrochloric acid (Fisher, technical grade, 35–38%) and 3 mL deionized water and cooling to room temperature. Subsequently, 1g of Ti_3AlC_2 powder was slowly added to the etching solution under stirring at room temperature and stirred for 15 hours. After etching process, the result suspension was washed with deionized water until a pH value of 6 was reached. 1.5 g of lithium chloride was adding to 30 ml deionized water and cooling to room temperature. The washed precipitate was transferred to the lithium chloride solution and stirring for 2 hours. After that, the suspension was washed with deionized water two times to remove the lithium chloride via centrifugation. The $Ti_3C_2T_x$ nanosheets were collected via centrifugation at 4,000 rpm for 5 minutes. The concentration of $Ti_3C_2T_x$ dispersion was measured by a certain amount of colloidal solution through a cellulose acetate filter paper (0.2-μm pore size) followed by drying under a vacuum at 70 °C overnight.

To synthesize the $Ti_3C_2T_x$/PB nanocomposite, 200 mg of Polyvinylpyrrolidone (average Mw=40000 g/mol) and 10 mL of the $Ti_3C_2T_x$ aqueous solution (1 mg/mL) were placed in a Teflon autoclave of 16-mL capacity. The pH of the mixture solution was adjusted to 1.5 by adding the hydrogen chloride acid solution. Oxygen in the mixture solution was removed by purging with argon for 30 minutes. Subsequently, the autoclave was sealed, heated to 90 °C, and maintained at this temperature for 90 minutes.

Supplementary Figures

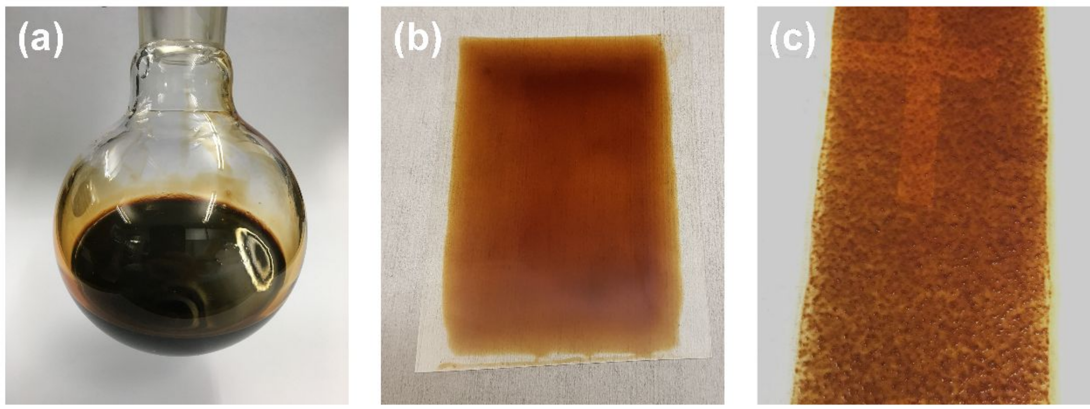

Figure S1. (a) The image of lignosulfonate/PVA/urea precursor solution, (b) The image of lignin/PVA/urea film prepared by blade-coating (60% lignosulfonate, 35% PVA, 5% urea), (c) The aggregated lignin/PVA/urea film where the content of urea is more than 5%.

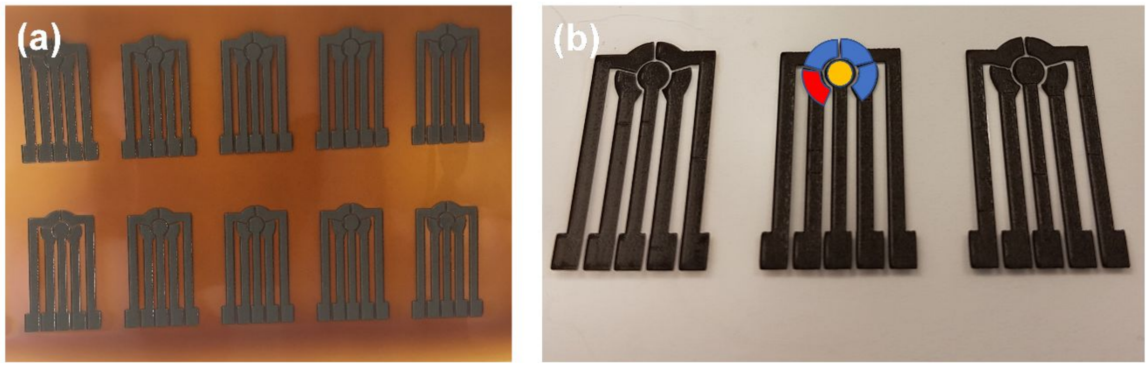

Figure S2. (a) The as-printed N-LSG electrodes patterns on the substrate, (b) The as-printed N-LSG electrode patterns after water lift-off process. The blue parts are the three working electrodes (the area is about 0.07 cm^2), the red part is the counter electrode, and the yellow part is the reference electrode.

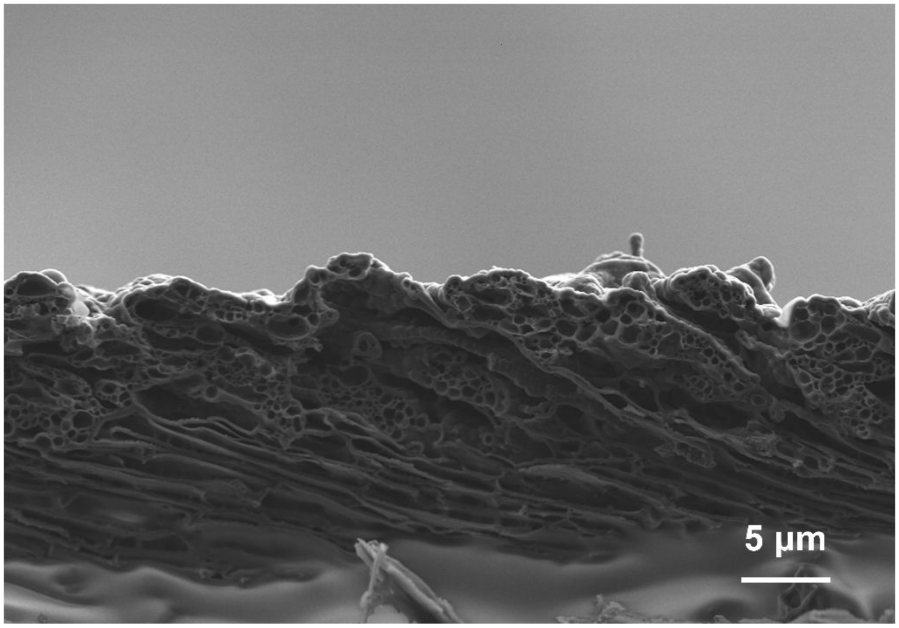

Figure S3. The tilted-view scanning electron microscopy (SEM) image of the N-LSG4.8 film.

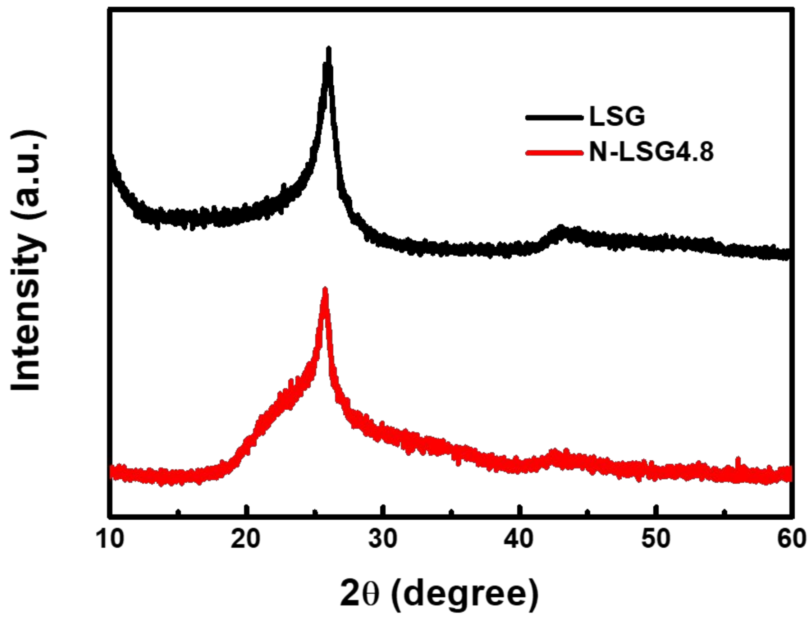

Figure S4. The XRD spectra of LSG and N-LSG4.8

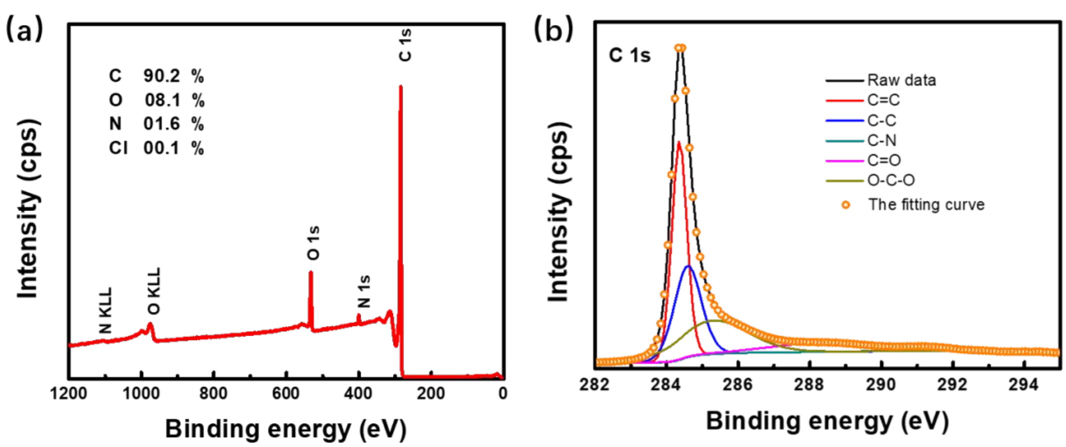

Figure S5. (a) XPS survey spectrum of N-LSG4.8, (b) C 1s high resolution XPS spectrum of N-LSG4.8 and the fitting curves.

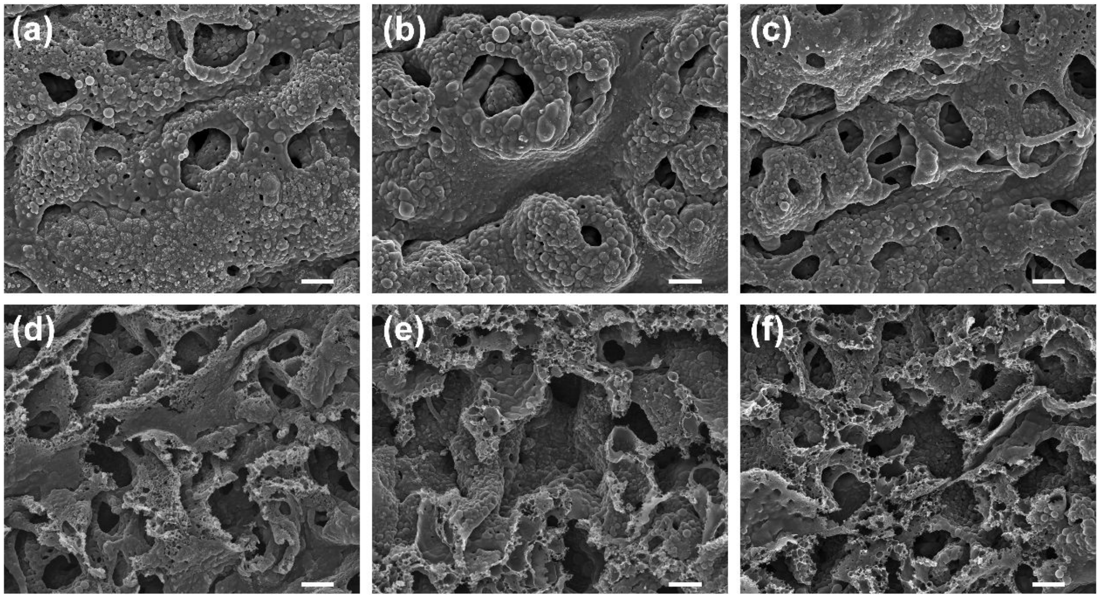

Figure S6. SEM images of the N-LSG electrodes after laser scribing process. (a) N-LSG2.8, (b) N-LSG3.2, (c) N-LSG3.6, (d) N-LSG-P4.0, (e) N-LSG-P4.4, (f) N-LSG-P4.8, all the scale bars are 4 μm.

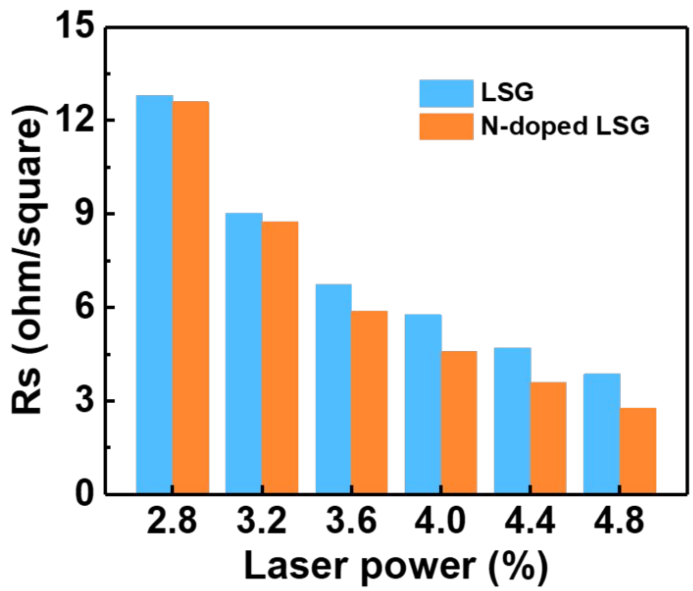

Figure S7. The sheet resistances of LSG and N-LSG films prepared with different CO_2 laser power.

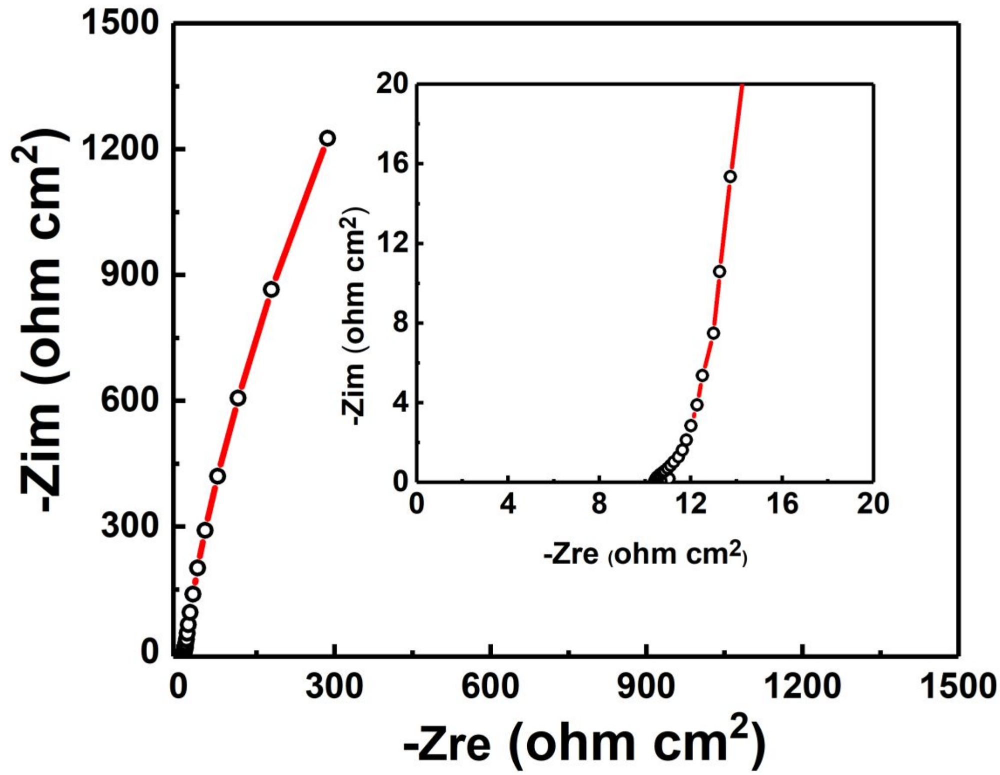

Figure S8. The Nyquist plot of N-LSG4.8 film with the inset focusing on the high-frequency region.

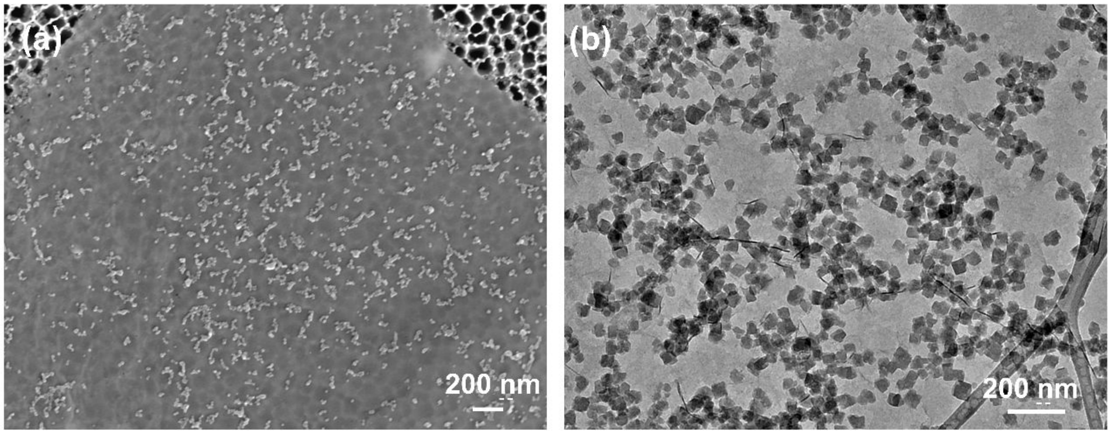

Figure S9. (a) The HRSEM image of the as-synthesized $Ti_3C_2T_x$/PB nanocomposites on porous alumina membrane, (b) The HRTEM image of the as-synthesized $Ti_3C_2T_x$/PB nanocomposites.

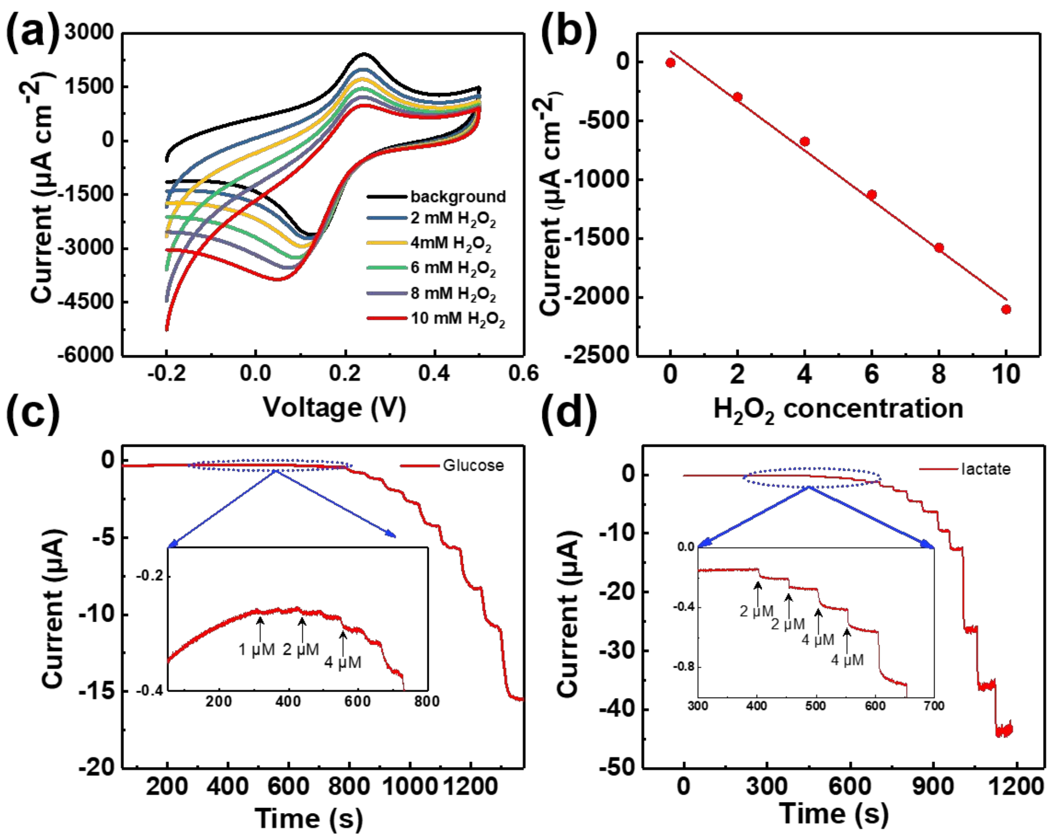

Figure S10. (a) The CV curves of the $Ti_3C_2T_x$/PB/N-LSG4.8 electrode showing the electroreduction of hydrogen peroxide at various concentrations. (b) Calibration curves derived from the currents measured at –0.1 V versus Ag/AgCl. (c) Chronoamperometric response of the Gox/$Ti_3C_2T_x$/PB/N-LSG4.8 glucose sensor to glucose from 1 μM to 1.1 mM. (d) Chronoamperometric response of the Lox/$Ti_3C_2T_x$/PB/CFMs lactate sensor to lactate from 2 μM to 800 μM. Both electrodes were biased at –0.1 V versus Ag/AgCl (home-made)

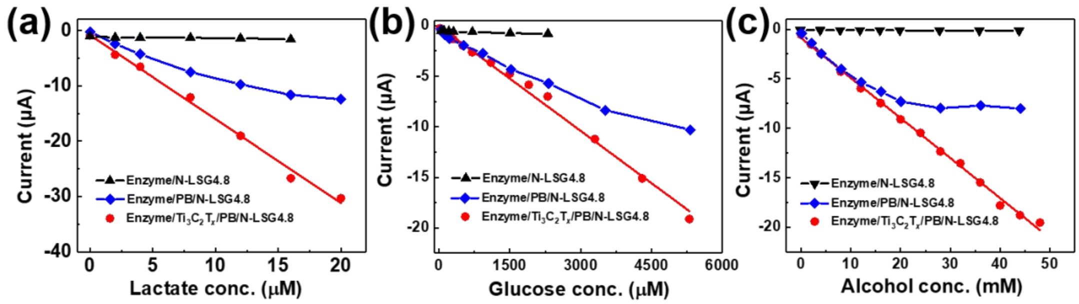

Figure S11. Calibration curves of enzyme/N-LSG4.8, enzyme/PB/N-LSG4.8 and enzyme/$Ti_3C_2T_x$/PB/N-LSG4.8 sensors. (a) glucose sensor, (b) lactate sensor, (c) alcohol sensor.

Table S1. Comparison of the performance of the enzyme/$Ti_3C_2T_x$/PB/N-LSG biosensors with the previously reported disposable biosensors towards the detection of glucose, lactate, and alcohol.

Sensors	Analyte	Linear range	Detection limit (μM)	Sensitivity	Potential (V)	Ref.
Gox/CoPC/SPCEs	Glucose	0.025 ~ 2 mM	25	13 μA $μM^{-1}$ cm^{-2}	0.5 (vs SCE)	1
GOD/CoPC/SPCEs	Glucose	0.2 ~ 5 mM	200	37.3 μA mM^{-1} cm^{-2}	0.5 (vs SCE)	2
GOD/Ir/Carbon/Gold	Glucose	0 ~ 15 mM	--	0.7 μA $mM^{-1}cm^{-2}$	0.25 (vs Ag/AgCl)	3
GOD/Cys/Au NPs/ITO	Glucose	0.04 ~ 4.8 mM	15	--	-0.1 (vs SCE)	4
Gox/SnO_2/Cellulose	Glucose	0.5~12 mM	--	13 μA $μM^{-1}$	-0.1	5
Lox/Pt/SPCEs	Lactate	0 ~ 1 mM	0.5	0.446 nA$μM^{-1}$	0.6 (vs Ag/AgCl)	6
Nafion/Lox/PB/SPCEs	Lactate	0.025~0.25	10	--	−0.05 (vs Ag/AgCl)	7

		mM				
Lox/Pt-CNF-PDDA/SPCEs	Lactate	25~1500 μM	11	36.8μA mM^{-1} cm^{-2}	0.5 (vs Ag/AgCl)	8
AOD/CoPC/SPCE	Alcohol	0.12 ~ 2.00 mM	--	1.2 μAmM^{-1}	0.4 (vs Ag/AgCl)	9
Gox/$Ti_3C_2T_x$/PB/N-LSG4.8	Glucose	10 ~ 5,300 μM	0.3	49.2 $\mu AmM^{-1}cm^{-2}$	-0.1	This work
Lox/$Ti_3C_2T_x$/PB/N-LSG4.8	Lactate	0 ~ 20 mM	0.5	21.6 $\mu AmM^{-1}cm^{-2}$	-0.1	This work
AOD/$Ti_3C_2T_x$/PB/N-LSG4.8	Alcohol	0 ~ 50 mM	--	5.78 $\mu AmM^{-1}cm^{-2}$	-0.1	This work

Table S2. Comparison of the performance of cellulosic materials using laser scribing for biochemical sensing

Sensors	Application	Linear range	Detection limit	Sensitivity	Ref.
LSCP/NN	Glucose sensor	0.8 -2.5 mM; 4.5 -15.2 mM	25 μM	3415 μA $mM^{-1}cm^{-2}$	10
GOD/CoPC/SPCE	Ascorbic	2.0 - 5.0 mM			11

s	acid				
	sensor	0.91 - 2.86			
	Caffeic	mM			
	acid				
	sensor	0.48 - 2.0 mM			
	Picric acid				
	sensor				
LSCP/CN	Glucose	0.001–7.96	0.03 μM	3626.6 μA	12
	sensor	mM		$mM^{-1}cm^{-2}$	
Fe_3O_4/MWCNTs/L	Cadmium	1- 200 μgL^{-1}	0.1μgL^{-1}		13
SG/CS/GCE	lead	1- 200 μgL^{-1}	0.07μgL^{-1}		
PBA-modified LSG	Aptamer		1 pM	-3.9 ± 0.3	14
	sensor			$\mu A\cdot cm^{-2}$	
Pt/LSG	Ascorbic	10 - 890 μM	6.1 μM	256 μA mM^{-}	15
	acid			$^{1}cm^{-2}$	
	sensor	0.5 - 56 μM	0.07 μM	6995.6μA	
	Dopamine			$mM^{-1}cm^{-2}$	
	sensor	1 - 63 μM	0.22 μM	8289μA mM^{-}	
	Uric acid			$^{1}cm^{-2}$	
	sensor				

Gox/$Ti_3C_2T_x$/PB/N-LSG4.8	Glucose sensor	10 ~ 5,300 μM	0.3	49.2 μAmM^{-1}cm^{-2}	This work
Lox/$Ti_3C_2T_x$/PB/N-LSG4.8	Lactate sensor	0 ~ 20 mM	0.5	21.6 μAmM^{-1}cm^{-2}	This work
AOD/$Ti_3C_2T_x$/PB/N-LSG4.8	Alcohol sensor	0 ~ 50 mM	--	5.78 μAmM^{-1}cm^{-2}	This work

REFERENCES

(1) Crouch, E.; Cowell, D. C.; Hoskins, S.; Pittson, R. W.; Hart, J. P. A Novel, Disposable, Screen-Printed Amperometric Biosensor for Glucose in Serum Fabricated Using a Water-Based Carbon Ink. *Biosens. Bioelectron.* **2005**, *21*, 712−718.

(2) Crouch, E.; Cowell, D. C.; Hoskins, S.; Pittson, R. W.; Hart, J. P. Amperometric, Screen-Printed, Glucose Biosensor for Analysis of Human Plasma Samples Using a Biocomposite Water-Based Carbon Ink Incorporating Glucose Oxidase. *Anal. Biochem.* **2005**, *347*, 17−23.

(3) Shen, J.; Dudik, L.; Liu, C. -C. An Iridium Nanoparticles Dispersed Carbon Based Thick Film Electrochemical Biosensor and Its Application for a Single Use, Disposable Glucose Biosensor. *Sens. Actuators, B.* **2007**,*125*, 106−113.

(4) Wang, J.; Wang, L.; Junwei Di, J.; Tu, Y. Disposable Biosensor Based on Immobilization of Glucose Oxidase at Gold Nanoparticles Electrodeposited on Indium Tin Oxide Electrode. *Sens. Actuators, B.* **2008**, *135*, 283−288.

(5) Mahadeva, S. K.; Kim, J. Conductometric Glucose Biosensor Made with Cellulose and Tin Oxide Hybrid Nanocomposite. *Sens. Actuators, B.* **2011**, *157*, 177−182.

(6) Patel, N. G.; Erlenkotter, A.; Cammann, K.; Chemnitius, C. C. Fabrication and Characterization of Disposable Type Lactate Oxidase Sensors for Dairy

Products and Clinical Analysis. *Sens. Actuators, B.* **2000**, *67*, 134−141.

(7) Petropoulos, K.; Piermarini, S.; Bernardini, S.; Palleschi, G.; Moscone, D. Development of a Disposable Biosensor for Lactate Monitoring in Saliva. *Sens. Actuators, B.* **2016**, *237*, 8−15.

(8) Lamas-Ardisana, P. J.; Loaiza, O. A.; Añorga, L.; Elena Jubete, E.; Borghei, M.; Ruiz, V.; Ochoteco, E.; Cabañero, G. Grande, H. J. Disposable Amperometric Biosensor based on Lactate Oxidase Immobilised on Platinum Nanoparticle-Decorated Carbon Nanofiber and Poly(diallyldimethylammonium chloride) films. *Biosens. Bioelectron.* **2014**, *56*, 345−351.

(9) Tu, D.; He, Y.; Rong, Y.; Wang, Y.; Li, G. Disposable L-lactate Biosensor Based on a Screen-Printed Carbon Electrode Enhanced by Graphene. *Meas. Sci. Technol.* **2016**, *27*, 045108. DOI: 10.1088/0957-0233/27/4/045108

(10) Hou, L.; Bi, S.; Lan, B.; Zhao, H.; Zhu, L.; Xu, Y.; Lu, Y. A novel and ultrasensitive nonenzymatic glucose sensor based on pulsed laser scribed carbon paper decorated with nanoporous nickel network. *Anal. Chim. Acta.*, **2019**, 1082, 165-175.

(11) de Araujo, W. R.; Frasson, C. M.; Ameku, W. A.; Silva, J. R.; Angnes, L.; Paixão, T. R. Single‐Step Reagentless Laser Scribing Fabrication of Electrochemical Paper‐Based Analytical Devices. *Angew. Chem. Int. Ed,* **2017,** 56, 15113-15117.

(12) Hou, L.; Zhao, H.; Bi, S., Zhu, L.; Xu, Y.; Lu, Y. Ultrasensitive and highly flexible nonenzymatic glucose biosensor based on laser-scribed carbon paper substrate. *Appl. Surf. Sci.*, **2019**, *465*, 320-331.

(13) Xu, Z.; Fan, X.; Ma, Q.; Tang, B.; Lu, Z.; Zhang, J.; Mo, G.; Ye, J.; Ye, J. A sensitive electrochemical sensor for simultaneous voltammetric sensing of cadmium and lead based on Fe_3O_4/multiwalled carbon nanotube/laser scribed graphene composites functionalized with chitosan modified electrode. *Mater. Chem. Phys.*, **2019,** *238*, 121877.

(14) Fenzl, C.; Nayak, P.; Hirsch, T.; Wolfbeis, O. S.; Alshareef, H. N.; Baeumner, A. J. Laser-scribed graphene electrodes for aptamer-based biosensing. *ACS Sens.*, **2017,** *2*, 616-620.

(15) Nayak, P.; Kurra, N.; Xia, C.; Alshareef, H. N. Highly efficient laser scribed graphene electrodes for on‐chip electrochemical sensing applications. *Adv. Electron. Mater.*, **2016,** *2*, 1600185.